

Skyrme RPA for nuclear resonances: trouble with magnetic modes

J. Speth,¹ P.-G. Reinhard,² V. Tselyaev,³ and N. Lyutorovich³

¹*Institut für Kernphysik, Forschungszentrum Jülich, D-52425 Jülich, Germany*

²*Institut für Theoretische Physik II, Universität Erlangen-Nürnberg, D-91058 Erlangen, Germany*

³*St. Petersburg State University, St. Petersburg, 199034, Russia**

(Dated: February 18, 2022)

We discuss major differences between electric and magnetic excitations in nuclei appearing in self-consistent calculation based on Skyrme energy-density functionals. Tools of analysis are Landau-Migdal parameters for bulk properties and RPA for resonance modes of ^{208}Pb as representative of finite nuclei. We show that the relation between the effective mass and the effective particle-hole interaction, well known in the Landau-Migdal theory, explains the success of self-consistent calculations of electric transitions in such approaches. This effect, however, does not automatically exist in the magnetic case. This calls for further developments of the Skyrme functional in the spin channel.

I. INTRODUCTION

Two different approaches have been successfully applied to calculation of nuclear resonance excitations. The traditionally most often used method of the first kind starts with a phenomenological single-particle model and an effective residual interaction. A widely used and powerful version is Migdal's theory of *Finite Fermi Systems* [1] based on Landau's *Theory of Fermi Liquids* [2]. This approach has been applied extensively to a broad range of nuclei, for reviews see [3]. In the second approach one starts with an effective energy density functional (EDF) which allows to derive the single particle model as well as the residual interaction. One of the most often used version is the Skyrme-Hartree-Fock (SHF) approach [4–7], for a review on SHF see [8]. Originally it was designed as a model for the nuclear ground state [9]. But soon it was also applied to compute self-consistently collective excitation states, especially giant resonances. The parameters of the early Skyrme EDF were predominately adjusted to ground state properties which does not a priori guarantee an appropriate particle-hole (ph) interaction. However, as incompressibility and symmetry energy are closely connected to the spin-independent isoscalar and isovector parts of the ph -interaction, in general the theoretical results were not so bad. In later parametrizations, also properties of excited states were included which improved the theoretical results compared to the data, see e.g. [10]. The Skyrme EDF turned out to be flexible enough to reproduce all collective modes with natural

parity. Most of the modern parameter sets use very similar values for the incompressibility K_∞ and symmetry energy a_{sym} . There is more variation in the choice of the effective mass m^* . As the effective mass has a heavy impact on the ph -spectrum, it is somewhat surprising that the RPA results of giant resonances and also of low-lying collective states are not very different. In that respect, it is instructive to learn from Landau Migdal (LM) theory; there it is known that the (spin-independent) isoscalar and isovector force parameters f_0 and f'_0 are correlated with the f_1 parameter quantifying effective mass, a feature similar to the *backflow* of quasi-particles in condensed matter [11]. With decreasing effective masses the isoscalar ph -interaction gets more attractive and the isovector ph -interaction becomes less repulsive thus correcting for the larger ph -energy spacing. We will show that this effect exists also for self-consistent calculations in the framework of Skyrme EDF.

Unfortunately there are no spin magnetic *bulk properties* known which are directly related to the spin dependent Landau-Migdal parameter g_0 and g'_0 . Moreover, there exists only one truly collective spin mode, namely the Gamow-Teller (GT)-resonance in neutron rich nuclei, which is related to the spin-isospin part of the residual ph -interaction. Therefore, the parameters which are most relevant for the spin-dependent part of the ph -interaction of the existing parametrizations were not yet adjusted to experimental properties with the exception of the two-body spin-orbit interaction. Bell and Skyrme introduced already more than 50 years ago a two-body spin-orbit term into the original ansatz in order to reproduce the single particle (sp) spin-orbit splitting [12]. Van Giai and Sagawa [13] modi-

* tselyaev@mail.ru

fied two Skyrme parametrizations where they considered the spin-dependent LM-parameter g_0 and g'_0 as additional constraints and calculated GT states in some doubly magic nuclei. Self-consistent calculations where the spin-dependent ph -interaction plays a role e.g. magnetic excitations, are very scarce. They came up only recently [14–16] and point toward insufficiency's of the Skyrme EDF as given. In the survey [16], the spin-relevant parameters of the Skyrme EDF were modified to reproduce the experimental data which amounts to a substantial readjustment of the LM parameters g_0, g'_0 .

The aim of this paper is to analyze the success of conventional Skyrme EDF for the natural parity (also called electrical) collective resonances and the failure in the spin channel. We use as tool the trends of LM parameters with effective mass. We start with the well settled and well working case of the electrical modes where we find that the “backflow effect” on the ph -interaction is the key to success. Then we apply the same strategy to LM parameters in the spin channel. In section II we give a short review into the Skyrme approach. In section III we present the relevant formulas of the Landau-Migdal approach where we especially emphasize the connection of the LM parameter with nuclear matter properties. In this connection we analyze the functional behavior of the spin-dependent and spin-independent LM parameter on the effective mass. Section IV contain the main result of our investigation. First we compare RPA and TBA results of electrical giant resonances with unperturbed ph energies for various Skyrme parametrizations. In the second part we show the corresponding results for the magnetic states using as example the 1^+ in ^{208}Pb . Finally we summarize and discuss our results in section V. In the Appendix A we discuss the density-dependence of f_0 and f'_0 which is crucial in the LM theory. As supplement to the section on giant resonances, we present in Appendix B RPA results for low-lying collective states. Appendices C and D contain the known formulas expressing the nuclear matter properties and the LM parameters in terms of the parameters of the Skyrme EDF.

II. THE SKYRME ENERGY FUNCTIONAL

The Skyrme energy functional consists of kinetic energy, Coulomb energy, pairing energy, and, as key entry, the Skyrme interaction energy. This is well documented in several reviews, see e.g. [8, 17]. We recall here just the core piece as far as is needed in following. The Skyrme

interaction energy is formulated in terms of a few nuclear densities and currents as are: density ρ_T , kinetic density τ_T , spin-orbit density \vec{J}_T , spin-tensor density \mathbb{J}_T , current \vec{j}_T , spin density \vec{s}_T , and spin kinetic density, where the index T stands for isospin ($T = 0$ or 1). It reads in commonly used form

$$\mathcal{E}_{\text{Sk}} = \sum_{T=0,1} \left(\mathcal{E}_T^{\text{even}} + \mathcal{E}_T^{\text{odd}} \right), \quad (1a)$$

$$\begin{aligned} \mathcal{E}_T^{\text{even}} = & C_T^\rho(\rho_0) \rho_T^2 + C_T^{\Delta\rho} \rho_T \Delta\rho_T + C_T^\tau \rho_T \tau_T \\ & + C_T^{\nabla J} \rho_T \nabla \cdot \vec{J}_T (+C_T^J \mathbb{J}_T^2), \end{aligned} \quad (1b)$$

$$\begin{aligned} \mathcal{E}_T^{\text{odd}} = & C_T^s(\rho_0) \vec{s}_T^2 + C_T^{\Delta s} \vec{s}_T \cdot \Delta \vec{s}_T \\ & + C_T^j \vec{j}_T^2 + C_T^{\nabla j} \vec{s}_T \cdot \nabla \times \vec{j}_T (+C_T^{sT} \vec{s}_T \cdot \vec{\tau}_T). \end{aligned} \quad (1c)$$

The terms employing the tensor spin-orbit densities are written in brackets to indicate that these terms are ignored in the majority of published Skyrme parametrizations. Only the time even part $\mathcal{E}_T^{\text{even}}$ is relevant for ground states of even-even nuclei. Time-odd nuclei and magnetic excitations are sensitive also to the time-odd part $\mathcal{E}_T^{\text{odd}}$. The parameters C_T^{type} for each term in the time-even part are adjusted independently, usually to a carefully chosen set of empirical data [8, 17]. A couple of different options are conceivable for the parameters of the time-odd terms which has consequences for the description of magnetic modes. This will be discussed in section IV C.

The original formulation of the Skyrme-Hartree-Fock (SHF) method was based on the concept of an effective interaction, coined the Skyrme force [4]. Modern treatments of SHF, however, start from a Skyrme energy-density functional as shown above. Nonetheless, the Skyrme force was the original motivation to develop the Skyrme functional and, being a zero-range interaction, displays an obvious similarity to the Landau-Migdal force. Its interaction part without spin-orbit and Coulomb terms has the form

$$E_{\text{Sk}}^{\text{int}} = E_{\text{Sk,dens}}^{\text{int}} + E_{\text{Sk,grad}}^{\text{int}}, \quad (2a)$$

$$\begin{aligned} E_{\text{Sk,dens}}^{\text{int}} = & \langle \Phi | t_0 (1 + x_0 \hat{P}_\sigma) \delta(\mathbf{r}_{12}) \\ & + \frac{t_3}{6} (1 + x_3 \hat{P}_\sigma) \rho^\alpha(\mathbf{r}_1) \delta(\mathbf{r}_{12}) | \Phi \rangle, \end{aligned} \quad (2b)$$

$$\begin{aligned} E_{\text{Sk,grad}}^{\text{int}} = & \langle \Phi | \frac{t_1}{2} (1 + x_1 \hat{P}_\sigma) \left(\delta(\mathbf{r}_{12}) \hat{\mathbf{k}}^2 + \hat{\mathbf{k}}^2 \delta(\mathbf{r}_{12}) \right) \\ & + t_2 (1 + x_2 \hat{P}_\sigma) \hat{\mathbf{k}} \delta(\mathbf{r}_{12}) \hat{\mathbf{k}} | \Phi \rangle, \end{aligned} \quad (2c)$$

where $\mathbf{r}_{12} = \mathbf{r}_1 - \mathbf{r}_2$ and $\hat{P}_\sigma = \frac{1}{2}(1 + \hat{\boldsymbol{\sigma}}_1 \hat{\boldsymbol{\sigma}}_2)$ is the spin-exchange operator. The $\hat{\mathbf{k}}$ stand for the momentum operators.

The Skyrme interaction (2) is not to be mixed with the residual interaction for computing excitation properties

within RPA, called henceforth *ph*-interaction. This residual interaction is deduced as second functional derivative of the Skyrme energy functional (1) [18] with respect to the local densities and currents it contains. As the functional (1) is composed of contact terms, the RPA residual interaction is a zero-range interaction. In that respect, it is very similar to the Landau-Migdal interaction, a feature which motivates a discussion of Skyrme RPA excitations in terms of Landau-Migdal (LM) parameters as we do here.

The Skyrme functional contains kinetic terms which leads to an effective nucleon mass m^* which differs from the bare mass m in the nuclear interior. This has consequences for many time-odd observables. For example, the current operator \hat{j}_q fails to satisfy the continuity equations if $m^* \neq m$. The non-trivial kinetic terms in the mean-field Hamiltonian call for a dynamical correction which reads [19]

$$\hat{j}_{\text{eff},q} = \hat{j}_q + \frac{m_q}{\hbar^2} \left(2b_1 \left[\rho_{\bar{q}} \hat{j}_q - \rho_q \hat{j}_{\bar{q}} \right] + b_4 \left[\rho_{\bar{q}} \vec{\nabla} \times \hat{\sigma}_q - \rho_q \vec{\nabla} \times \hat{\sigma}_{\bar{q}} \right] \right) \quad (3)$$

where q denotes proton or neutron, \bar{q} the nucleon with opposite isospin, the coefficients b_1 and b_4 are defined in Ref. [18]. This correction is crucial, e.g., in the computation of transition strengths for giant resonances [20]. It exemplifies the backflow effect known from the theory of Fermi liquids [21]. The same correction is also required for the magnetic current [22]. We will see below that a similar backflow-like correction appears also for the residual interaction in RPA.

III. LANDAU-MIGDAL THEORY

The Landau-Migdal theory of excitations in fermionic systems was developed originally in the context of Fermi fluids [23–25] and extended later to finite nuclei [1]. The LM *ph*-interaction is restricted to the Fermi surface where it depends only on the angle between the momenta \mathbf{p} and \mathbf{p}' of the $1ph$ states before and after the collision. The *ph*-interaction in momentum space is a function $F^{ph}(\mathbf{p}, \mathbf{p}')$ times spin and isospin operators. The momentum dependence can be expanded in terms of Legendre polynomials in the dimensionless combination $\mathbf{p} \cdot \mathbf{p}' / |\mathbf{p}| |\mathbf{p}'|$ [23–25]. The coefficients of this expansion are called LM parameters. The leading order ($l = 0$) of the Legendre polynomial is a constant which gives rise in \mathbf{r} -space to a delta function ($F^{ph}(1, 2) = \delta(\mathbf{r}_{12})$) similar

as the leading term in the Skyrme interaction. The term next to leading order ($l = 1$) is proportional to $(\mathbf{p} \cdot \mathbf{p}')$. To deal better with the finite size of the nuclei, one often introduces density dependent LM parameters in the following way [1]:

$$f(\rho) = f^{\text{ex}} + (f^{\text{in}} - f^{\text{ex}}) \frac{\rho_0(r)}{\rho_0(0)}$$

where f^{ex} stands for the exterior region of the nucleus and f^{in} for the interior. However, the density dependence of the Skyrme *ph*-interaction differs from that form which would require a discussion of its own [26]. Thus we concentrate on the interior region, the nuclear bulk properties, and drop the upper index “in” in the following.

A. Dimensionless Landau-Migdal (LM) parameters

The expansion parameters have the same dimension as the interaction, namely energy \times length³, which varies strongly with system size. To obtain a dimensionless measure of interaction strength, it is customary to single out a pre-factor having this dimension. A natural measure of length³ is the inverse of bulk density ρ_0 . Thus Migdal uses as normalization factor the derivative $C_0^{(\text{Migdal})} = d\epsilon_F/d\rho_0 = \pi^2 \hbar^2 / (mk_F) \approx 300 \text{ MeV fm}^3$ which applies to models using bare nucleon mass m [1]. Landau et al. take a similar normalization factor, however, half of that and keeping the effective nucleon mass m^* in the definition [2]. This amounts to parametrize the RPA interaction in terms of LM parameters F_l , G_l as

$$F^{ph}(\mathbf{p}, \mathbf{p}') = C_0^* \sum_l P_l\left(\frac{\mathbf{p} \cdot \mathbf{p}'}{k_F^2}\right) \left[F_l + F_l' \tau_1 \cdot \tau_2 + G_l \sigma_1 \cdot \sigma_2 + G_l' \sigma_1 \cdot \sigma_2 \tau_1 \cdot \tau_2 \right] \quad (4a)$$

$$C_0^* = \frac{\pi^2 \hbar^2}{2m^* k_F} \approx 150 \text{ MeV fm}^3 \frac{m}{m^*}. \quad (4b)$$

This normalization has the advantage that the condition for stable RPA modes becomes simply $F_0 > -1$ and it is most suited for self-consistent nuclear models where effective mass $m^* \neq m$ plays a role. Many publications in the context of the Skyrme-Hartree-Fock (SHF) model use this normalization. Still, Migdal’s definition using a fixed normalization factor is also often used, particularly in the empirical LM model. Thus we discuss both definition side by side. However, we want to avoid the trivial, but distracting, factor two in the comparison and use for that

LM parameters	
effective-mass normalization	bare-mass normalization
$F_0 = \frac{K_\infty}{6T_F^*} - 1$	$f_0 = \frac{m}{m^*} F_0 = \frac{K_\infty}{6T_F} - \frac{m}{m^*}$
$F'_0 = \frac{3a_{\text{sym}}}{T_F^*} - 1$	$f'_0 = \frac{m}{m^*} F'_0 = \frac{3a_{\text{sym}}}{T_F} - \frac{m}{m^*}$
$F_1 = 3 \left(\frac{m^*}{m} - 1 \right)$	$f_1 = \frac{m}{m^*} F_1 = 3 \left(1 - \frac{m}{m^*} \right)$
$F'_1 = 3 \left((1 + \kappa_{\text{TRK}}) \frac{m^*}{m} - 1 \right)$	$f'_1 = \frac{m}{m^*} F'_1 = 3 \left(1 + \kappa_{\text{TRK}} - \frac{m}{m^*} \right)$

NMP	LM parameters	
	consistent norm.	fixed norm.
$\frac{K_\infty}{6} =$	$T_F^* (1 + F_0)$	$T_F \left(\frac{m}{m^*} + f_0 \right)$
$\frac{m}{m^*} =$	$\frac{1}{1 + \frac{F_1}{3}}$	$1 - \frac{f_1}{3}$
$3a_{\text{sym}} =$	$T_F^* (1 + F'_0)$	$T_F \left(\frac{m}{m^*} + f'_0 \right)$
$1 + \kappa_{\text{TRK}} =$	$\frac{m}{m^*} \left(1 + \frac{F'_1}{3} \right)$	$\frac{m}{m^*} + \frac{f'_1}{3}$

TABLE I. The two forms of LM parameters (5) and (4) and their relation to nuclear matter parameters (NMP). Upper block: definition of LM parameters in terms of NMP. Lower block: NMP computed from LM parameters. The kinetic energies T_F and T_F^* are defined in equation (6).

the normalization form

$$F^{ph}(\mathbf{p}, \mathbf{p}') = C_0 \sum_l P_l \left(\frac{\mathbf{p} \cdot \mathbf{p}'}{k_F^2} \right) \left[f_l + f'_l \tau_1 \cdot \tau_2 + g_l \sigma_1 \cdot \sigma_2 + g'_l \sigma_1 \cdot \sigma_2 \tau_1 \cdot \tau_2 \right] \quad (5a)$$

$$C_0 = \frac{\pi^2 \hbar^2}{2mk_F} \approx 150 \text{ MeV fm}^3. \quad (5b)$$

Henceforth we call the choice (5) "bare-mass normalization" and the choice (4) "effective-mass normalization". Each one of the two definitions has its advantages and disadvantages. The bare-mass normalization (5) produces a measure of strength of residual interaction term by term comparable across SHF parametrizations with different m^*/m . The effective-mass normalization (4) produces comparable effects of the residual interaction (stability condition, excitation energies). The reason is that different interaction strengths are required to compensate the impact of different m^*/m , similar as in the backflow effect [11], see eq. (3).

B. Relation to nuclear matter properties (NMP)

First we look at nuclear matter properties (NMP) which provide a unique characterization of the basic nuclear response properties in the volume: incompressibility K_∞ , effective mass m^*/m , symmetry energy a_{sym} , and Thomas-Reiche-Kuhn (TRK) sum rule enhancement κ_{TRK} . The first two are isoscalar response properties and the second two are isovector properties. The κ_{TRK} is a way to parametrize the isovector effective mass [8]. All four are the response properties in the excitations channels with natural parity. The NMP for spin modes are not nearly that well developed, particularly because the data basis on magnetic excitations is not strong enough to support unambiguous extrapolation to bulk. Thus we concentrate first on the group of natural parity modes. In many of the expressions for NMP appears the (effective) nucleon mass frequently in a combination which is the kinetic energy T_F of bulk matter. To simplify notations, we introduce for it the abbreviations

$$T_F = \frac{\hbar^2 k_F^2}{2m}, \quad T_F^* = \frac{\hbar^2 k_F^2}{2m^*} = \frac{m}{m^*} T_F. \quad (6)$$

Columns 1 and 2 in the upper block of Table I list the LM parameters in effective-mass and bare-mass normalization together with their relations to NMP. The parameters in effective-mass normalization (column 1) demonstrate nicely the interplay between mean field (terms with the leading contribution "1") and the residual interaction (terms with F's). With bare-mass normalization, the terms representing the mean field are in most cases m/m^* which takes into account that self-consistent models can stretch or squeeze the level spacing and the residual interaction thus has to work against the modified level density, similar to the backflow effect eq. (3) for currents. The lower block shows, in turn, how NMP are computed from LM parameters. Again, the place where the effective mass enters makes the crucial difference between bare-mass normalization and effective-mass normalization. Particularly noteworthy are the entries for f_1 and f'_1 , or F_1 and F'_1 respectively. These show that self-consistent models establish an intimate connection between these first-order parameters and effective masses m/m^* and κ_{TRK} . One is not allowed to change one without consistently modifying the other. This counterplay is also reflected in the backflow correction eq. (3) for flow observables.

The dimensionless LM parameters allow also to express the stability conditions for excitations modes. These are

$F_0^{(l)} > -1$ for effective-mass normalization or $\frac{m^*}{m} f_0^{(l)} > -1$ for bare-mass normalization, and similarly $F_1^{(l)} > -3$ or $\frac{m^*}{m} f_1^{(l)} > -3$ for $l = 1$ (where the compact upper index (l) means that this holds for F as well as for F' type parameters). The stability conditions look more natural for effective-mass normalization while one has first to undo the m/m^* factor in case of bare-mass normalization.

As argued above, the parameters f_0, f'_0 , defined with bare-mass normalization, represent directly the strength of the residual interaction. The first two lines of Table I show a clear dependence $f_0^{(l)} = c - m/m^*$ where c is some constant: The smaller m^* , the stronger the isoscalar interaction and the weaker the isovector one which is necessary to counterweight the lower level density at the Fermi surface (the “backflow effect” for the RPA interaction). The upper panel of Fig. 1 shows these trends for the natural-parity channel together with the values for $f_0^{(l)}$ from a representative set of well working Skyrme parametrizations. The results from the realistic parametrizations fit nicely to the analytical trend and so confirm the need to properly counterweight the level-spreading effect of the effective mass.

For completeness, we show in Table II the NMP and corresponding LM parameters for a selection of Skyrme parametrizations with systematically varied NMP [10, 27]. The detailed expressions of the LM parameters in terms of the parameters of the Skyrme interaction (2) are given in Appendix D.

C. The spin channel

Now we turn to the spin channel and we will see that the case is dramatically different. A first problem is that we do not have well established NMP for spin response and that spin modes in finite nuclei are not as prominent as giant resonances of natural parity. Both together leaves the empirical calibration of the residual interaction in the spin channel an open problem [16]. Second, in many mean-field models, the spin channel is determined once the natural-parity response is fixed. For example, relativistic mean-field models tie spin properties and kinetic properties closely together [28]. This need not to be beneficial if it turns out that the “predictions” thus obtained are wrong. That is the aspect which we will address here for the case of the SHF model.

The spin properties in the Skyrme EDF’s are not uniquely fixed. These leaves different options for its choice [29] which lead to rather different result for the

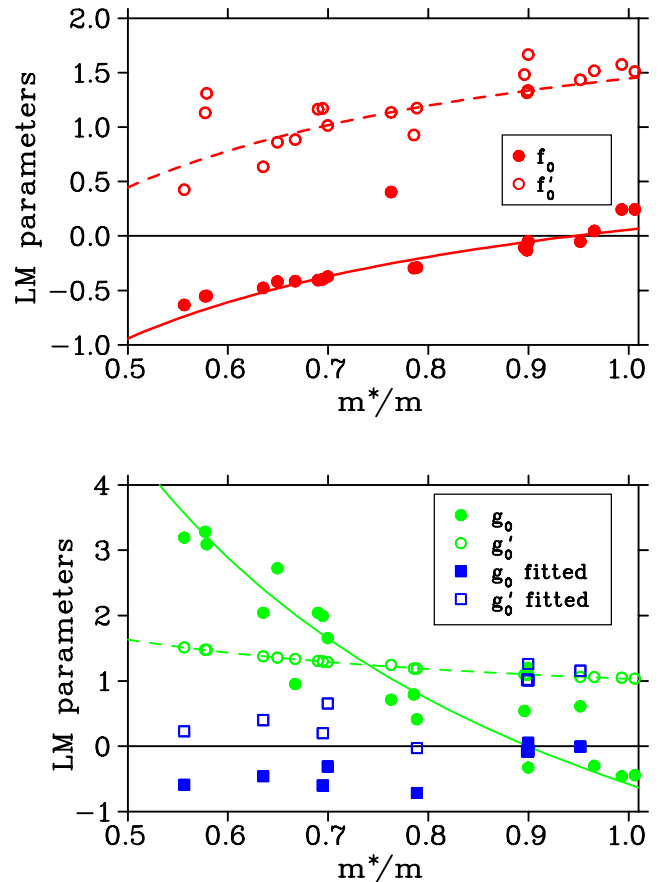


FIG. 1. Dependence of the LM parameters on the effective mass m^*/m . Upper panel: f_0 (filled red circles), f'_0 (open red circles) derived from the collection of the most widely used Skyrme parametrizations given in Table I of [16]. The lines indicate the trends $a + bm^*/m$ of f_0 (solid line) and f'_0 (dashed line), computed with the NMP of SV-bas (Table II) except for m^*/m which is varied. Lower panel: g_0 (filled green circles) and g'_0 (open green circles) for the same Skyrme parametrizations. The lines indicate again the trends $a + bm^*/m$ (solid line for g_0 , dashed line for g'_0). Also shown are the adjusted LM spin parameters which reproduce the magnetic dipole states in ^{208}Pb (g_0 as filled blue squares, g'_0 as open blue squares) for the corresponding Skyrme parametrizations taken from [16].

LM parameters of G type:

1. One can understand SHF as stemming from the effective density-dependent zero-range interaction (2) which determines all spin terms from the given

EDF	m^*/m	K_∞ (MeV)	κ_{TRK}	a_{sym} (MeV)	F_0	F'_0	F_1	f_0	f'_0	f_1
SV-bas	0.90	233	0.4	30	-0.05	1.20	-0.30	-0.05	1.34	-0.33
SV-sym34	0.90	234	0.4	34	-0.04	1.50	-0.30	-0.05	1.67	-0.33
SV-mas10	1.00	234	0.4	30	0.06	1.45	0.00	0.06	1.45	0.00
SV-mas07	0.70	234	0.4	30	-0.26	0.71	-0.90	-0.37	1.01	-1.29
SV-K218	0.90	218	0.4	30	-0.12	1.18	-0.30	-0.13	1.32	-0.34
SV-m64k6	0.64	241	0.6	27	-0.30	0.40	-1.09	-0.48	0.64	-1.72
SV-m56k6	0.56	255	0.6	27	-0.35	0.24	-1.33	-0.63	0.43	-2.39

TABLE II. Nuclear matter parameters and spin-independent LM parameters, in both normalizations.

natural-parity partners and its NMP. By combining the formulas of Appendices C and D this yields

$$g_0 + g_1 = -(3 + 3\kappa_{\text{TRK}}) - \frac{3a_{\text{sym}} - 2\frac{B}{A}}{T_F} + \frac{26}{5} \frac{m}{m^*}, \quad (7a)$$

$$g'_0 + g'_1 = \frac{B}{A} \frac{1}{T_F} + \frac{3}{5} \frac{m}{m^*}. \quad (7b)$$

2. Even when taking the viewpoint of option 1, most actual parametrizations drop the tensor spin-orbit terms “tensor terms” $\propto \vec{J}^2$ which are generated as partners of the kinetic terms in the force definition of the SHF functional. This yields the variant

$$g_0 = -(3 + 3\kappa_{\text{TRK}}) - \frac{3a_{\text{sym}} - 2\frac{B}{A}}{T_F} + \frac{26}{5} \frac{m}{m^*}, \quad (8a)$$

$$g'_0 = \frac{B}{A} \frac{1}{T_F} + \frac{3}{5} \frac{m}{m^*}, \quad (8b)$$

$$g_1 = 0, \quad (8c)$$

$$g'_1 = 0. \quad (8d)$$

3. One can dismiss the concept of a force and start from an energy-density functional in which case the spin terms are constrained only by the requirement of Galilean invariance leaving a couple of terms open. These can be adjusted independently from the terms of natural parity and so allow for more flexible tuning of magnetic modes. This has been done, e.g., in [16]. No closed formula for the G parameters can be given here.
4. As in option 3, one can start from a Skyrme energy-density functional, but now freeze the spin terms by the requirement of “minimal Galilean invariance” which means to discard all spin terms which are not fixed by Galilean invariance [29]. This yields for the G parameters the trivial result

$$G_0 = 0, \quad G'_0 = 0, \quad G_1 = 0, \quad G'_1 = 0. \quad (9)$$

Let us first investigate the option 2 which assumes an underlying Skyrme force and thus predicts the properties in the spin channel from the known properties in the natural-parity channel. The LM parameters are thus given by eqs. (8). The trend with m^* is of the form $g_0^{(\prime)} = a^{(\prime)} + b^{(\prime)}m/m^*$ where $a^{(\prime)}$ and $b^{(\prime)}$ are some constant. This looks similar to the trend for the $f_0^{(\prime)}$. The crucial difference is, however, that the mass dependence comes with a plus sign. The trend is visualized in the lower panel of Fig. 1. Note that the deviation of the open green circles from the dashed line is negligible because the first term in the right-hand side of Eq. (8b) is practically the same for all parametrizations. We see that the $g_0^{(\prime)}$ parameters increase with decreasing m^*/m which goes the wrong way because it is counter-productive for compensating the decrease of level density in the single-particle spectrum. The options 1 and 2 which understand the SHF model as an effective interaction is thus to be discarded for principle reasons.

This result has also been found at several places from studying magnetic excitations in finite nuclei, see e.g. [15, 16]. In [16], the spin-parameters in the Skyrme functional had been adjusted freely to M1 modes in finite nuclei. This corresponds to option 3 in the above list. The resulting $g^{(\prime)}$ are shown as squares in Fig. 1. The g_0 stay close to zero for the parametrizations with $m^*/m \approx 1$. The g'_0 a bit larger, still being small. Both show a slight tendency to decrease with decreasing m^*/m which is the expected trend. This empirical result allows also the option 4 for g_0 . This is not so clear for g'_0 . To be on the safe side, the option option 3 turns out to be the recommended option.

IV. LM PARAMETERS AND RESONANCE EXCITATIONS IN ^{208}Pb

A. The random phase approximation (RPA)

In this section, we are going to investigate excitation properties in a finite nucleus, namely ^{208}Pb . The most often used method for calculating excitation properties in nuclear physics is the RPA and its various extended versions. There exists numerous different derivations which all lead to the same basic RPA equation [20]:

$$(\epsilon_{\nu_1} - \epsilon_{\nu_2} - \Omega_m) \chi_{\nu_1\nu_2}^{(m)} = (n_{\nu_1} - n_{\nu_2}) \sum_{\nu_3\nu_4} F_{\nu_1\nu_4\nu_2\nu_3}^{\text{ph}} \chi_{\nu_3\nu_4}^{(m)}. \quad (10)$$

The $\chi_{\nu_1\nu_2}^{(m)}$ are the ph excitation amplitudes in the single-particle configuration space, F^{ph} is the ph -interaction, ϵ_ν are the sp energies and Ω_m the excitation energies of the nucleus. There exist two different methods to determine the input data:

(I) The phenomenological shell model approach where one starts with an empirically adjusted single particle model and parametrizes the ph -interaction. A very successful approach in this connection is the Landau-Migdal theory [1, 30].

(II) The self-consistent approach where one starts with an effective energy-density functional (EDF) from which one derives the single-particle quantities as well as the ph -interaction [18]. In this paper we discuss particularly Skyrme type EDF's.

There exist various extended versions of RPA which include configurations beyond $1ph$, e.g., phonon coupling in time blocking approximation (TBA), for details see [31, 32]. Most of these models employ again the basic ph interaction F^{ph} . Thus no new parameters have to be introduced.

The RPA equation (10) shows that there are two basic ingredients which determine at the end the excitation spectra: the $1ph$ energies $\epsilon_p - \epsilon_h$ and the ph -interaction F^{ph} . The energies are determined with the ground state which leaves little leeway for tuning. The ph -interaction is exclusively seen in the excitations and most of their impact can be characterized in simple terms through the LM parameters as done throughout this paper.

B. Giant resonances

We start with excitations of natural parity, also called electrical modes. Their spectral distribution in a heavy nucleus as ^{208}Pb and in channels with low angular momentum L is dominated by one strong peak called a giant resonance. Most prominent are the isoscalar giant monopole resonance (GMR), the isoscalar giant quadrupole resonance (GQR), and the the isovector giant dipole resonance (GDR). All three resonances can be characterized by one number, the resonance energy, which we will use now for the looking at trends and relations to LM parameters. Fig. 2 collects giant-resonance properties together with the leading LM parameters (upper panels) for a variety of Skyrme parametrizations with systematically varied NMP, see Table II. In order to check the impact of complex configurations beyond RPA, we compare resonance energies from RPA with those from TBA. The differences in the energies are small while the resonance width is significantly affected by the complex configurations in TBA [16, 33, 34]. At present, we focus on resonance energies and can ignore the small difference between RPA and TBA. Together with the resonance energies, we shows also the average $1ph$ energies ε_{ph} (averaged over the $1ph$ spectrum weighted by the transition operator of each mode). The difference between ε_{ph} and the resonance energy visualizes the impact of the ph -interaction and that is obviously considerable, strongly attractive in the isoscalar modes (lower block) and strongly repulsive in the isovector modes (upper block). Note that the Skyrme parametrizations are sorted in order of decreasing effective mass with $m^*/m = 1$ to the left and the lowest $m^*/m = 0.56$ to the right. It is obvious that the ε_{ph} increase while the resonance energies change comparatively little. The increase of ε_{ph} is largely compensated by a properly counter-acting trend of the ph -interaction. This trend can be nicely read off from the LM parameters shown in the upper panels. It is the same as shown already in Fig. 1 and we learn from the present figure that the trend $\propto c - m/m^*$ which is typical for the LM parameters in the natural parity channels is exactly what is needed to compensate the dilution of $1ph$ spectra with decreasing effective mass.

Although the variations of resonance energies are small as compared to the effects of the ph -interaction, there is important systematics in it. They demonstrate the known intimate connection between NMP and resonance energies [10]: the giant monopole resonance (GMR) is

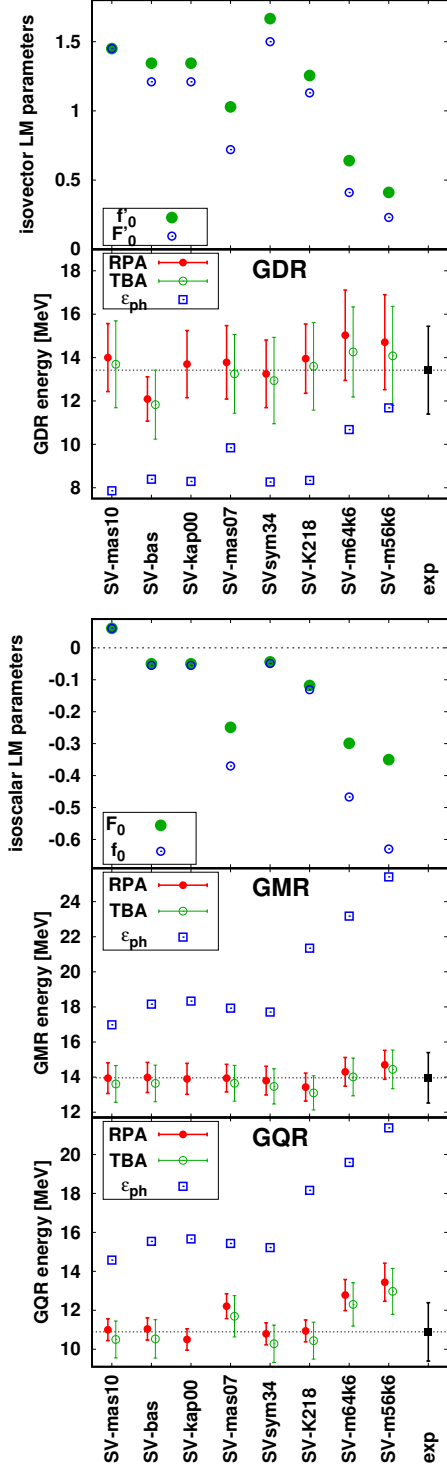


FIG. 2. Collection of giant-resonance properties in ^{208}Pb together with LM parameters for a representative set of Skyrme parametrizations covering a variation of all four NMP [10, 27]. Upper block: isovector properties, LM parameters in upper panel and RPA properties (resonance energies, average $1ph$ energies) in the lower panel. Lower block: isoscalar properties, LM parameters in upper panel, RPA properties in middle and lower panel. In addition to RPA results, also results from TBA are shown.

related exclusively to the incompressibility K_∞ , the giant dipole resonance (GDR) to the sum rule enhancement κ_{TRK} , and the giant quadrupole resonance (GQR) to the effective mass m^*/m . These trends are much more subtle than the dramatic trends for the ϵ_{ph} . It is remarkable how the interplay between mean-field and ph -interaction can recover the subtle trends.

C. The magnetic case

In case of magnetic modes, there are no isoscalar spin dependent resonances known which suggests that the spin-dependent isoscalar ph -interaction is weak. On the other hand, there exist collective neutron-particle proton-hole resonances in nuclei with neutron excess. The best known resonances are the (1^+) Gamow-Teller resonances. The corresponding unperturbed $1ph$ -strength is shifted to higher energies which is a clear indication that the spin-isospin ph -interaction has to be strongly repulsive which was confirmed in Ref. [35] comparing the experimental GT resonance in ^{208}Pb together with two theoretical results. However, the Gamow-Teller resonances reside in a regime where effective energy functionals are most probably insufficient. We thus concentrate on the low-energy M1 modes.

The 1^+ -states in ^{208}Pb are a nice example for the behavior of the spin-dependent isoscalar and isovector interaction. There is an isoscalar state at $E_1 = 5.84$ MeV which is close to the uncorrelated proton and neutron spin-orbit doublets $\epsilon_{ph}^\pi = 5.55$ MeV and $\epsilon_{ph}^\nu = 5.84$ MeV and a couple of isovector 1^+ states with the mean energy $E_2 = 7.39$ MeV. This again shows that the spin-dependent isoscalar ph -interaction is weak and the spin-dependent isovector ph -interaction is strongly repulsive. In a recent publication by our group [16] we investigated these 1^+ states in the framework of RPA using various Skyrme parameter sets with different effective masses. There we took the Skyrme functional as derived from a Skyrme interaction with all spin terms fixed by the model, option 2 of section IIIC. Fig. 3 shows the RPA results of the isoscalar and isovector M1 modes together with the unperturbed $1ph$ energies. The trends of the $1ph$ energies are the same as for the giant resonances in Fig. 2 and the computed M1 energies amplify this trend driving the RPA results far off the experimental values. This demonstrates on the grounds of the empirical results that the option to take the Skyrme interaction literally is inappropriate for magnetic modes. In the paper [16], we

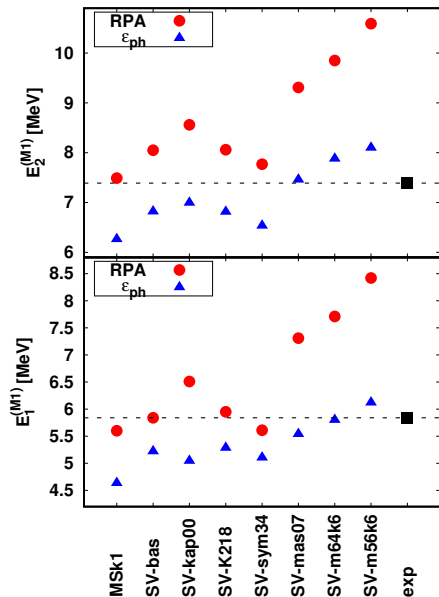


FIG. 3. Energies of the lower ($E_1^{(M1)}$; lower figure) and higher ($E_2^{(M1)}$; upper figure) M1 states in ^{208}Pb calculated within RPA for a selection of different Skyrme parametrizations (full red circle) compared with the experimental values (black box and faint dashed line). Also shown are the energy of the unperturbed ε_{ph} from proton spin-orbit pair (lower figure) and neutron spin orbit pair (upper figure), indicated by blue triangles.

had also considered the spin terms in the Skyrme functional as free for independent calibration (option 3 in section IIIC). The energies of the M1 modes reproduce, by construction, the experimental energies and are thus not shown in the figure. The non-trivial message in this respect is that one can do such fine tuning of spin modes without destroying the overall quality of the parametrization.

V. CONCLUSION

We explored in this paper the general pattern and trends of Landau-Migdal (LM) parameters in connection with the self-consistent models using the Skyrme energy-density functional (EDF). As starting point, we reviewed the channel of natural-parity excitations. The well known experience is that giant resonances are well described for several Skyrme EDF's although they can have quite different effective nucleon masses. This is surprising because changing the effective mass changes energy spacing of particle-hole (ph) states dramatically. The fact

that giant resonances do not change that much implies that the change in ph spacing is compensated by a corresponding change in the residual ph -interaction: smaller effective mass gives larger ph spacings and thus the ph -interaction has to be more attractive (isoscalar channel) or less repulsive (isovector channel). In the present paper, we studied in quantitative detail these correlations between ph -spacing and strength of residual ph -interaction for Skyrme EDF's. The latter were quantified in terms of LM parameters which depend, apart from m^*/m , only on five nuclear matter parameters (Fermi momentum k_F , bulk binding energy B/A , incompressibility K_∞ , symmetry energy a_{sym} and Thomas-Reiche-Kuhn sum rule enhancement κ_{TRK}). Modern Skyrme parametrizations have only a moderate dispersion in these parameters leaving close correlations between m^*/m and LM parameters. As expected, with decreasing effective m^*/m the LM parameter f_0 (isoscalar) becomes more attractive and f'_0 (isovector) less repulsive and the trend has exactly the right amount to guarantee that the energies of isoscalar and isovector electrical giant resonance are well reproduced by Skyrme parametrizations with different effective masses.

Then we turned to magnetic modes, i.e. excitations with unnatural parity. The situation is found to be completely different. First of all, there exist no well settled magnetic bulk properties which may be included in the fitting of the EDF parameters. This leaves several options for determining the EDF in the spin channel. Either one derives the spin parameters from the zero-range Skyrme force as done traditionally, or one dismisses all terms which are not required by Galilean invariance, or takes spin-sensitive data to calibrate them. Second, there are no strong collective magnetic resonances known with the exception of the GT-resonances in neutron rich nuclei which, however, is likely to lie outside the range of a description by Skyrme EDF's. Thus we take as reference here the strongest isoscalar and isovector M1-states in ^{208}Pb . The isoscalar state is close to the two (experimental) spin-orbit partners while the more fragmented isovector states are shifted by about two MeV to higher energies. Taking the definition of spin parameters in the EDF from the Skyrme force runs into difficulties for M1 resonances in ^{208}Pb . The RPA results do not describe the data and there do not exist the clear correlations between unperturbed ph states and RPA results. The main point of our paper is that this problem is already apparent from bulk properties, namely looking at the trends

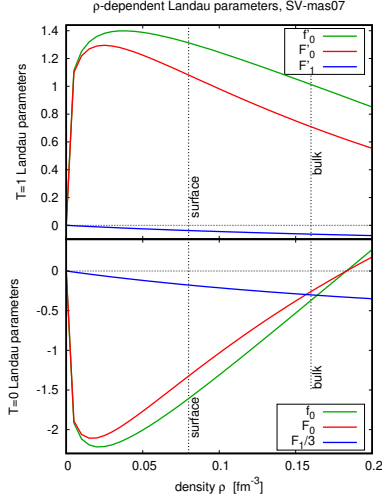


FIG. 4. Density dependence of the isovector LM parameters f'_0 , F'_0 , F'_1 in the upper part and the isoscalar LM parameters f_0 , F_0 , F_1 in the lower part. The quantities are derived from the Skyrme parametrization SV-mas07.

of the spin dependent LM parameters g_0 and g'_0 as function of m^*/m . These trends are going into the opposite direction as the well performing LM parameters f_0 and f'_0 in the natural-parity channel. This provides, already at the level of bulk properties, a strong argument against the definition of a Skyrme EDF by a Skyrme force. The argument is corroborated by the observation that the values of g_0 and g'_0 differ substantially from those obtained previously by a fit to the empirical M1 resonances. This altogether demonstrates once again that the spin channel in Skyrme EDF's is different and still require careful calibration.

ACKNOWLEDGMENTS

This research was carried out using computational resources provided by the Computer Center of St. Petersburg State University.

Appendix A: On the density dependence of LM parameters

As said above, the LM theory for finite nuclei as well as the SHF model augment the LM parameters with some density dependence. Fig. 4 shows the density dependent LM parameters for the parametrization SV-mas07. Near

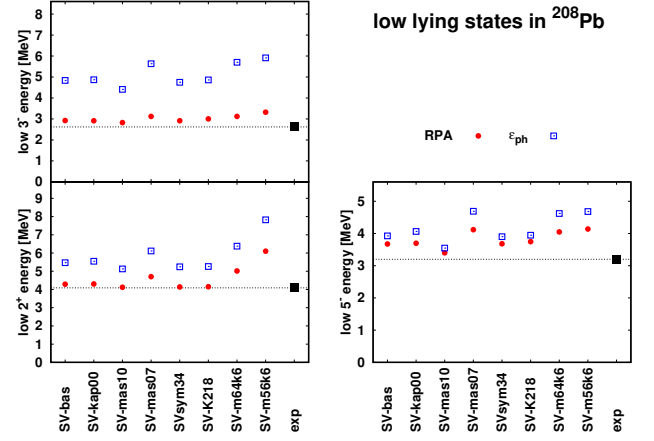


FIG. 5. Energies of the first excited 3^- , 5^- and 2^+ states in ^{208}Pb calculated within RPA. We compare the results of different Skyrme parametrizations with the data. We also show the energy of the lowest unperturbed $1ph$ -pair for each multipolarity indicated by blue quads.

bulk density, it is linear similar to LM theory. But it differs dramatically from linear behavior at low densities.

Appendix B: Low-lying collective electric states

In Fig. 5 we present the energies of the first 3^- , 5^- and 2^+ states in ^{208}Pb calculated in RPA with various Skyrme parametrizations. For each parameter set also the energy of the lowest unperturbed $1ph$ state in the corresponding channel is given. From numberless calculations, e.g. Ref. [36], we know that the lowest 3^- state is the most collective state in ^{208}Pb . Many $1ph$ state within the $1\hbar\omega$ -shell contribute coherently which gives rise to the well known large transition probability and large energy shift. This is nicely demonstrated in the left upper section of Fig. 5 where all $1ph$ energies stay far above the finally lowest state (red dots). To the 5^- state also many $1ph$ states within the $1\hbar\omega$ -shell contribute but obviously in this case the ph -interaction is too weak to generate a strongly collective state. Therefore the shift from the unperturbed states is much smaller and reaches in no case the experimental line. For the 2^+ states only two neutron and two proton $1ph$ states within the $1\hbar\omega$ -shell contribute. On the other hand many $1ph$ states from the $1\hbar\omega$ -shell contribute and give rise to a relatively large transition moment. The energy shifts are smaller than in the 3^- case but reaches in most cases the experimental

value. The down-shift of the energy comes along with an enhanced transition moment (not shown here) which is another realization of collectivity (coherent superposition of many $1ph$ states). Most collective resonance in that respect is the 3^- state and it is no surprise that we see, again, the same feature as for the giant resonances, namely that the uncoupled $1ph$ energies change with Skyrme force while the RPA results are practically the same. From this we conclude that for collective states the *back-flow* is an important corrective mechanism.

the following form (see, e.g., Ref. [37])

$$0 = \frac{2}{5}T_F + \frac{3}{8}t_0\rho_{\text{eq}} + \frac{1}{16}t_3(\alpha+1)\rho_{\text{eq}}^{\alpha+1} + \frac{1}{16}\Theta_s k_F^2 \rho_{\text{eq}}, \quad (\text{C1})$$

$$-B/A = \frac{3}{5}T_F + \frac{3}{8}t_0\rho_{\text{eq}} + \frac{1}{16}t_3\rho_{\text{eq}}^{\alpha+1} + \frac{3}{80}\Theta_s k_F^2 \rho_{\text{eq}}, \quad (\text{C2})$$

$$K_\infty = \frac{6}{5}T_F + \frac{9}{4}t_0\rho_{\text{eq}} + \frac{3}{16}t_3(\alpha+1)(3\alpha+2)\rho_{\text{eq}}^{\alpha+1} + \frac{3}{4}\Theta_s k_F^2 \rho_{\text{eq}}, \quad (\text{C3})$$

$$a_{\text{sym}} = \frac{1}{3}T_F - \frac{1}{8}t_0(2x_0+1)\rho_{\text{eq}} - \frac{1}{48}t_3(2x_3+1)\rho_{\text{eq}}^{\alpha+1} + \frac{1}{24}(2\Theta_s - 3\Theta_v)k_F^2 \rho_{\text{eq}}, \quad (\text{C4})$$

$$\kappa_{\text{TRK}} = \frac{m\rho_{\text{eq}}}{4\hbar^2}\Theta_v, \quad (\text{C5})$$

$$\frac{m}{m^*} = 1 + \frac{m\rho_{\text{eq}}}{8\hbar^2}\Theta_s, \quad (\text{C6})$$

where $\rho_{\text{eq}} = 2k_F^3/3\pi^2$ is the equilibrium density, $T_F = \hbar^2 k_F^2/2m$,

$$\Theta_s = 3t_1 + (5 + 4x_2)t_2, \quad (\text{C7})$$

$$\Theta_v = (2 + x_1)t_1 + (2 + x_2)t_2. \quad (\text{C8})$$

Appendix D: Landau-Migdal parameters

The Landau-Migdal parameters deduced from the Skyrme EDF (2) are related with the parameters of this functional by the formulas (see, e.g., Refs. [13, 38])

$$C_0^* F_0 = \frac{3}{4}t_0 + \frac{1}{16}t_3(\alpha+1)(\alpha+2)\rho_{\text{eq}}^\alpha + \frac{1}{8}k_F^2[3t_1 + (5 + 4x_2)t_2], \quad (\text{D1})$$

$$C_0^* F_0' = -\frac{1}{4}t_0(1 + 2x_0) - \frac{1}{24}t_3(1 + 2x_3)\rho_{\text{eq}}^\alpha + \frac{1}{8}k_F^2[(1 + 2x_2)t_2 - (1 + 2x_1)t_1], \quad (\text{D2})$$

$$C_0^* F_1 = -\frac{1}{8}k_F^2[3t_1 + (5 + 4x_2)t_2], \quad (\text{D3})$$

$$C_0^* F_1' = -\frac{1}{8}k_F^2[(1 + 2x_2)t_2 - (1 + 2x_1)t_1], \quad (\text{D4})$$

$$C_0^*(G_0 + G_1) = -\frac{1}{4}t_0(1 - 2x_0) - \frac{1}{24}t_3(1 - 2x_3)\rho_{\text{eq}}^\alpha, \quad (\text{D5})$$

$$C_0^*(G_0' + G_1') = -\frac{1}{4}t_0 - \frac{1}{24}t_3\rho_{\text{eq}}^\alpha, \quad (\text{D6})$$

$$C_0^* G_1 = \frac{1}{8}[(1 - 2x_1)t_1 - (1 + 2x_2)t_2]k_F^2, \quad (\text{D7})$$

$$C_0^* G_1' = \frac{1}{8}(t_1 - t_2)k_F^2, \quad (\text{D8})$$

with C_0^* as defined in Eq. (4b). Note that $G_1 = G_1' = 0$ independently of Eqs. (D7) and (D8) for the Skyrme EDFs in which the \mathbf{J}^2 terms are omitted (see Ref. [39] for more detail).

Appendix C: Nuclear matter properties

Within the density functional theory, the properties of symmetric infinite nuclear matter (the Fermi momentum k_F , the total binding energy per nucleon B/A , the nuclear matter incompressibility K_∞ , the symmetry energy a_{sym} , the enhancement factor of the Thomas-Reiche-Kuhn sum rule κ_{TRK} , and the effective mass m^*) are determined by the parameters of the energy-density functional. In the case of Skyrme EDF (2) the respective equations have

-
- [1] A. B. Migdal, *Theory of Finite Fermi Systems and Application to Atomic Nuclei* (Wiley, New York, 1967).
- [2] L. D. Landau, E. M. Lifshitz, and L. P. Pitajevski, “Course of Theoretical Physics 9–Statistical Physics,” (Pergamon press, Oxford, 1980).
- [3] J. Speth, E. Werner, and W. Wild, Phys. Rep. **33**, 127 (1977).
- [4] T. H. R. Skyrme, Nucl. Phys. **9**, 615 (1959).
- [5] J. W. Negele and D. Vautherin, Phys. Rev. C **C5**, 1472 (1972).
- [6] J. W. Negele and D. Vautherin, Phys. Rev. C **C11**, 1031 (1975).
- [7] K. F. Liu and G. E. Brown, Nucl. Phys. A **265**, 385 (1976).
- [8] M. Bender, P.-H. Heenen, and P.-G. Reinhard, Rev. Mod. Phys. **75**, 121 (2003).
- [9] D. Vautherin and D. Brink, Phys. Rev. C **5**, 626 (1972).
- [10] P. Klüpfel, P.-G. Reinhard, T. J. Bürvenich, and J. A. Maruhn, Phys. Rev. C **79**, 034310 (2009).
- [11] J. Bardin and J. R. Schrieffer, in *Progress in low Temperature Physics*, Vol. 3, edited by C. J. Gorter (North-Holland, 1961) p. 170.
- [12] J. S. Bell and T. H. R. Skyrme, Philos. Mag. **1**, 1055 (1956).
- [13] N. Van Giai and H. Sagawa, Phys. Lett. B **106**, 379 (1981).
- [14] P. Vesely, J. Kvasil, V. O. Nesterenko, W. Kleinig, P.-G. Reinhard, and V. Y. Ponomarev, Phys. Rev. C **80**, 031302(R) (2009).
- [15] V. O. Nesterenko, J. Kvasil, P. Vesely, W. Kleinig, P.-G. Reinhard, and V. Y. Ponomarev, J. Phys. G: Nucl. Part. Phys. **37**, 064034 (2010).
- [16] V. Tselyaev, N. Lyutorovich, J. Speth, P.-G. Reinhard, and D. Smirnov, Phys. Rev. C **99**, 064329 (2019).
- [17] J. Erler, P. Klüpfel, and P. G. Reinhard, J. Phys. G **38**, 033101 (2011).
- [18] P.-G. Reinhard, Ann. Phys. (Leipzig) **504**, 632 (1992).
- [19] A. Repko and J. Kvasil, Acta Phys. Pol. B Proc. Suppl. **12**, 689 (2019).
- [20] P. Ring and P. Schuck, *The Nuclear Many-Body Problem* (Springer, New York, Heidelberg, Berlin, 1980).
- [21] D. Pines and P. Nozières, *The Theory of Quantum Liquids* (W A Benjamin, New York, 1966).
- [22] J. A. McNeil, R. D. Amado, C. J. Horowitz, M. Oka, J. R. Shepard, and D. A. Sparrow, Phys. Rev. C **34**, 746 (1986).
- [23] L. D. Landau, JETP **3**, 920 (1957).
- [24] L. D. Landau, JETP **5**, 101 (1957).
- [25] L. D. Landau, JETP **8**, 70 (1959).
- [26] J. Speth, S. Krewald, F. Grümmer, P. G. Reinhard, N. Lyutorovich, and V. Tselyaev, Nucl. Phys. A **928**, 17 (2014).
- [27] N. Lyutorovich, V. I. Tselyaev, J. Speth, S. Krewald, F. Grümmer, and P.-G. Reinhard, Phys. Rev. Lett. **109**, 092502 (2012).
- [28] P.-G. Reinhard, Rep. Prog. Phys. **52**, 439 (1989).
- [29] K. J. Pototzky, J. Erler, P.-G. Reinhard, and V. O. Nesterenko, Eur. Phys. J. A **46**, 299 (2010).
- [30] J. Speth and J. Wambach, in *Electric and Magnetic Giant Resonances in Nuclei*, Vol. International Review of Nuclear Physics, Vol. 7, edited by J. Speth (World Scientific, 1991) pp. 2–87.
- [31] V. I. Tselyaev, Phys. Rev. C **75**, 024306 (2007).
- [32] V. Tselyaev, N. Lyutorovich, J. Speth, S. Krewald, and P.-G. Reinhard, Phys. Rev. C **94**, 034306 (2016).
- [33] V. Tselyaev, N. Lyutorovich, J. Speth, and P.-G. Reinhard, Phys. Rev. C **96**, 024312 (2017).
- [34] V. Tselyaev, N. Lyutorovich, J. Speth, and P.-G. Reinhard, Phys. Rev. C **97**, 044308 (2018).
- [35] T. Wakasa, M. Okamoto, M. Dozono, K. Hatanaka, M. Ichimura, S. Kuroita, Y. Maeda, H. Miyasako, T. Noro, T. Saito, Y. Sakemi, T. Yabe, and K. Yako, Phys. Rev. C **85**, 064606 (2012).
- [36] P. Ring and J. Speth, Phys. Lett. B **44**, 477 (1973).
- [37] E. Chabanat, P. Bonche, P. Haensel, J. Meyer, and R. Schaeffer, Nucl. Phys. A **627**, 710 (1997).
- [38] J. Margueron, J. Navarro, and N. Van Giai, Phys. Rev. C **66**, 014303 (2002).
- [39] T. Lesinski, M. Bender, K. Bennaceur, T. Duguet, and J. Meyer, Phys. Rev. C **76**, 014312 (2007).